Food Innovation and Advances

ARTICLE

Open Access

https://doi.org/10.48130/fia-0026-0031

Food Innovation and Advances **2026**, 5(3): 362–371

Tunable physicochemical properties, oral sensation, and digestive behavior of gelatin/κ-carrageenan-beeswax-based bigel beads: effects of fabrication parameters and phase ratio

Yujie Zhao[1], Jiangliu Song[1], Jingyi Yang[1], Yujuan Jin[2], Guoping Li[3], Jinfang Liu[1] and Like Mao[1*]

[1] *Key Laboratory of Healthy Beverages, China National Light Industry, College of Food Science and Nutritional Engineering, China Agricultural University, Beijing 100083, China*

[2] *School of Light Industry Science and Engineering, Beijing Technology and Business University, Beijing 100048, China*

[3] *School of Materials Science and Technology, Beijing Institute of Technology, Beijing 100081, China*

* Correspondence: likemao@cau.edu.cn (Mao L)

Abstract

In this study, we optimized the fabrication of bigel beads using a combination of orthogonal experiments and response surface methodology, with special focus on refining the gelling bath parameters and extrusion techniques. We systematically investigated the influence of the oil–water phase ratio on the properties of bigel beads and comprehensively evaluated their performance in simulated oral processing and gastrointestinal digestion. Our key findings were that the gelling bath composed of 75% ethanol and 0% Tween at 0 °C achieved the highest gelation rate (0.9882), while the optimal extrusion parameters that yielded the maximum sphericity (0.9751) were a pump rate of 0.13 mL/min, height 0.93 cm, and temperature 65 °C. The elevated oil-phase content significantly enhanced both the particle size and sphericity of the bigel beads, transformed the bigel type from O/W to bi-continuous, and increased the hardness and cohesiveness. Furthermore, a higher oleogel percentage exacerbated frictional interactions during simulated mastication, compromised structural stability, and consequently promoted the release of free fatty acids. These results provide novel insights into the fabrication protocols and structure–function relationships of bigel beads, contributing to the development of functional food materials.

Keywords: Bigel beads, Gelling bath, Extrusion, Sphericity, Friction

Citation: Zhao Y, Song J, Yang J, Jin Y, Li G, et al. 2026. Tunable physicochemical properties, oral sensation, and digestive behavior of gelatin/κ-carrageenan-beeswax-based bigel beads: effects of fabrication parameters and phase ratio. *Food Innovation and Advances* 5(3): 362–371 https://doi.org/10.48130/fia-0026-0031

Introduction

Gels, defined as semisolid systems containing a liquid phase entrapped within a three-dimensional cross-linked network, represent a versatile class of materials with diverse applications[1]. They are broadly classified into two primary types: hydrogels, in which water constitutes the liquid phase, and oleogels, which utilize organic solvents as the dispersed liquid component[2]. Building on this framework, bigels have emerged as an innovative biphasic material integrating both hydrogel and oleogel phases, existing in three distinct structural configurations—oleogel-in-hydrogel, hydrogel-in-oleogel, and bi-continuous phases—and can be fabricated through a simple mixing process[3,4]. Because of the advantages of both hydrogels and oleogels, such as enhanced stability, improved nutritional profiles, and tunable adaptability to diverse applications, bigels have rapidly gained attention in recent scientific and industrial research[5–7].

The performance of bigels is deeply influenced by the hydrogel/oleogel ratio. Zheng et al.[3] reported that bigels with higher oleogel content displayed improved mechanical properties, such as an elevated storage modulus, stiffness, and fracture stress. Conversely, Martins et al.[8] observed that bigels with higher hydrogel volume fractions exhibited greater hardness. These seemingly contradictory findings underscore the complexity of bigel systems, because their performance is modulated not only by component ratios but also by interfacial interactions and microstructural features, highlighting the need for systematic studies to unravel how bigel architecture determines the functional properties. Gel beads, a well-characterized spherical colloidal system valued for its consumer appeal, bioactive material protection capabilities, and potential in dysphagia management[9–11], has sparked wide interest.

The methods of preparing gel beads, such as extrusion, spray, and spinning techniques, have been studied extensively, with simple dripping or extrusion emerging as the most widely used approach[10]. However, the properties of gel beads are highly sensitive to the fabrication parameters, particularly gelling bath conditions and extrusion techniques. Despite extensive research on conventional gel beads (e.g., calcium alginate systems), in which factors such as gelation temperature, solution viscosity, and dripping height have been linked to microstructure and shape control[12–14], studies focusing on bigel beads remain limited. Critical gaps persist in understanding how preparation techniques influence the properties of gel beads, hindering the development of tailored bigel bead systems. Against this backdrop, the objectives of this study were twofold: (1) optimize the preparation process to fabricate bigel beads with high gelation efficiency and sphericity using orthogonal experiments (for gelling bath parameters) and response surface methodology (RSM, for extrusion techniques); and (2) characterize the key properties of these optimized bigel beads, such as appearance, microstructure, mechanical behavior, tribological characteristics, and *in vitro* digestion behavior, across varying hydrogel/oleogel ratios. We hypothesized that an optimized preparation process would enhance the gelation rate and sphericity and variations in the hydrogel/oleogel ratio would significantly modulate the properties of bigel beads. The findings

from this work are expected to expand the application scope of bigel beads and advance the development of novel functional food products.

Materials and methods

Materials

κ-Carrageenan was purchased from Azelis Co., Ltd. (Shanghai, China). Beeswax was obtained from Suzhou Cross-century Biotechnology Co., Ltd. (Suzhou, China). Rapeseed oil was provided by Yihai Kerry Arawana Holdings Co., Ltd. (Shanghai, China). Tween 20 was bought from Sinopharm Chemical Reagent Co., Ltd. (Shanghai, China). Walnut oil was the product of Guanghua Modern Agriculture Co., Ltd. (Kashi, China). K_2HPO_4 was offered by Macklin Co. Ltd. (Shanghai, China). $NaHCO_3$, NaCl, $CaCl_2$, HCl, and NaOH were purchased from Beijing Chemical Works Co., Ltd. (Beijing, China). Pepsin, pancreatin, pancreatic lipase, bile salt, α-amylase, and mucin were bought from Sigma Aldrich (St. Louis, MO, USA).

Preparation of bigel beads

Beeswax (15%, w/w) and κ-carrageenan (2.0%, w/w) were completely dissolved in rapeseed oil and deionized water at 85 °C, respectively. Tween was added at a final concentration of 2.5% (w/w) in emulsions. The oil phase and water phase (in the ratio 2:3) were mixed and homogenized at 65 °C using a T18 Ultra Turrax mixer (IKA, Germany) at 5,000 rpm for 2 min followed by 7,000 rpm for 3 min. The emulsions were kept at 65 °C after ultrasonication for 5 min.

To obtain bigel beads, the emulsions were dropped through a syringe (1.6 mm i. d.) into an ethanol solution using a peristaltic pump to achieve stable bead formation. Once the beads were formed, they were kept in the gelling media for 30 s for cross-linking. They were then washed with distilled water three times and dried before storing at 4 °C for 12 h for further analysis.

Optimization of the gelling bath

Before conducting the orthogonal tests, three variables (ethanol concentration, bath temperature, and Tween concentration) were tested at five levels to analyze the effect of each factor on the the gelation rate of bigel beads and determine the preliminary range. One factor was changed in each experiment. The specific conditions were as follows: ethanol concentration (0, 25%, 50%, 75%, and 100%), bath temperature (−8, −4, 0, 4, and 8 °C), and Tween concentration (0, 0.5%, 1.0%, 1.5%, and 2.0%). Subsequently, the gelling bath was further optimized using orthogonal tests with three levels for each factor. The experimental design for the orthogonal tests is given in Supplementary Table S1.

Optimization of the processing technique using the Box-Behnken design (BBD)

The effects of peristaltic pump rate, dripping height, and transporting temperature on the sphericity of bigel beads were analyzed, and three variables were tested at five levels. One factor was changed in each experiment. The specific conditions were as follows: peristaltic pump rate (0.05, 0.10, 0.15, 0.20, and 0.25 mL/min), dripping height (0.5, 1.0, 1.5, 2.0, and 2.5 cm), and transporting temperature (60, 65, 70, 75, and 80 °C). Subsequently, BBD was used for structuring the experimental data. Response surface methodology (RSM) was applied to the experimental data using Design-Expert and multiple regression analysis was performed. The initial range of the three factors was determined based on the findings from the single-factor experiments. Each factor was assigned three levels: −1, 0, and 1. Detailed information on the experimental design is provided in Supplementary Table S2.

The statistical significance of the terms in the regression equations was assessed using analysis of variance (ANOVA) for each response. The adequacy of the models was determined based on model analysis, lack-of-fit test, coefficient of determination (R^2), and adjusted-R^2 analysis. The correlation between the response and independent variables can be readily seen in the contour and three-dimensional (3D) graphic surface plots, providing insights into the optimum levels and most influential variables for the sphericity of bigel beads. The contour graphs illustrated whether the interactions between corresponding variables were significant, while the response surface graphs (3D) demonstrated the change in response values with variable alterations[15]. In these graphs, a single variable was kept constant, enabling variation of the remaining two variables within the experimental parameters.

Preparation of bigel beads using the optimized fabrication process

For improved density of the network structure and higher gel strength, gelatin (10.0%, w/w) and κ-carrageenan (0.5%, w/w) were used in water phase[16], and walnut oil was used for the oil phase. Before homogenizing, the oil phase and water phase were mixed in the ratios 4:6, 3:7, and 2:8. The emulsions were sterilized at 85 °C for 30 min and dropped from 0.93 cm at 65 °C into a 75% (w/w) edible alcohol solution at 0 °C to achieve stability, using a peristaltic pump operated at a speed of 0.13 mL/min. The beads containing 20%, 30%, and 40% oil phase were denoted as O-2, O-3, and O-4, respectively. A proportion of the beads were added into yogurt and stored at 4 °C. The other steps were the same as mentioned in "Preparation of bigel beads".

Characterization of bigel beads

Size, sphericity, and gelation rate

The average diameter was obtained by measuring the diameter of at least 100 fresh beads with the software ImageJ, and the gauss fitting was performed. The shape of the beads was determined from the sphericity factor according to Eq. (1):

$$\text{Sphericity} = \frac{d_{\min}}{d_{\max}}, \tag{1}$$

where d_{max} and d_{min} are, respectively, the maximum and minimum diameters of the beads.

The gelation rate was calculated according to Eq. (2):

$$\text{Gelation rate} = \frac{m_1}{m_2}, \tag{2}$$

where m_1 and m_2 are, respectively, the mass of bigel beads with sphericity ≥ 0.75 and the mass of all bigel beads[9].

Microstructure

An inverted confocal laser scanning microscope (Zeiss LSM880, Zeiss, Inc., Germany) was used to examine the distribution of oil droplets in cross sections according to a published method[9].

https://doi.org/10.48130/fia-0026-0031

Textural properties

A uniaxial compression test was carried out on individual beads using a CT3 texture analyzer (Brookfield, Middleboro, MA, USA) according to a previous method[9].

Simulated oral processing and digestion

Tribology

Bigel beads containing different percentages of oil phase were added into yogurt at concentrations of 6% (w/w) and 10% (w/w). The composition of the artificial saliva was kept the same as in the previous study[17]. The yogurt containing bigel beads was homogenized with artificial saliva in the ratio 2:1 (w/w) using a T18 Ultra Turrax mixer to simulate oral processing[18].

A HAKKE MARS iQ Air rheometer (Thermo Scientific Inc., Karlsruhe, Germany) was used to perform the tribological measurements. A normal tension of 1.0 N was used. Friction coefficients (μ, unitless) were recorded at an entrainment speed ranging from 0.1 to 939.8 mm/s[19].

Free fatty acid release during simulated digestion

Simulated saliva contained 0.111 g/L NaCl, 1.492 g/L KCl, 3.948 g/L $NaHCO_3$, 0.278 g/L $CaCl_2$, 0.096 g/L $MgCl_2$•$6H_2O$, 1.5 g/L mucin, 2 g/L α-amylase. pH of the saliva was adjusted to 6.8 using 1 mol/L HCl. The simulated gastric fluid (SGF, pH 2.0) was composed of 1 mol/L HCl, 0.2% NaCl (w/w), and 0.32% pepsin (w/w). The simulated intestinal fluid (SIF, pH 7.0) was composed of 0.68% K_2HPO_4 (w/w), 0.8775% NaCl (w/w), 0.04% pancreatin (w/w), 0.32% pancreatic lipase (w/w), and 1% bile salt (w/w).

A three-stage digestion model was used. All experiments were conducted at 37 °C. *Mouth phase*: The simulated saliva fluid (10 mL) was mixed with the bigels (2.0 g) to start mouth-phase digestion. The mixture was incubated for 10 min. Then, 2.5 mL of the mixture was collected. *Gastric phase*: 20 mL of SGF was added into the mixed samples after mouth-phase digestion to start gastric-phase digestion. The mixture was incubated for 120 min. During the simulated gastric phase, the mixture was sampled (2.5 mL) every 30 min. *Intestinal phase*: 20 mL of SIF was added into the mixed samples after gastric-phase digestion to start intestinal-phase digestion. The mixture was incubated for 120 min. During the simulated intestinal phase, the mixture was sampled (2.5 mL) every 30 min. The cumulative release rate of free fatty acid (FFA) was calculated for each sampling time according to Eq. (3):

$$\mathrm{FFA}(\%) = 100 \times V_{\mathrm{NaOH}} \times m_{\mathrm{NaOH}} \times M_{\mathrm{lipid}} / (w_{\mathrm{lipid}} \times 2), \quad (3)$$

where V_{NaOH} is the volume of NaOH required to neutralize the FFA produced (L), m_{NaOH} is the molarity of the NaOH used (in M), w_{lipid} is the total mass of triacylglycerol oil initially present in the digestion cell (in g), and M_{lipid} is the average molecular weight of the triacylglycerol oil (g/mol)[20].

Statistical analysis

All measurements were conducted in triplicate, and the resulting data were presented as mean ± standard deviation. SPSS 23 was used for ANOVA, with a significance level of $p < 0.05$.

Results and discussion

Effect of the gelling bath on bigel beads

To assess the effect of ethanol on the gelation rate of bigel beads, various concentrations were tested (Table 1). The gelling bath without ethanol showed the lowest gelation rate (0.3323). Increasing the ethanol concentration to 75% enhanced the gelation rate to its maximum (0.9693), indicating that addition of an appropriate concentration of ethanol improved the gelation rate. Literature suggests that ethanol has the ability to promote the gelation of carrageenan because of its hydrophobic effect[21,22]. Specifically, ethanol stabilized the intermolecular interactions and produced dense strands to facilitate carrageenan assembly, leading to a more rigid and denser microstructure[22]. Consequently, it enhanced gelatinization, thereby improving the shape retention of the bigel beads. However, when the ethanol concentration reached 100%, the gelation rate declined (0.8474). This phenomenon can be attributed to ethanol's osmotic effect: the high ethanol concentration created osmotic pressure, causing water to migrate from the beads to the medium[23]. Consequently, bead shrinkage occurred and the gelation rate was reduced. In the previous study, when the konjac glucomannan (KGM) gel was immersed in ethanol solution, it lost approximately 70% of its weight as the ethanol concentration exceeded 60%[24]. Additionally, ethanol could act as a fixative that increased the gel's network packing and chain entanglement, further contributing to shrinkage[24]. Therefore, the ethanol concentration must be carefully controlled within an intermediate range to optimize the sphericity and gelation rate of bigel beads.

As shown in Table 1, increasing the gelling temperature from −8 to 0 °C enhanced the gelation rate from 0.8418 to a maximum value of 0.9844. It was probably because the gelling bath had lower viscosity at higher temperature[25], and lower viscosity diminished the impact forces when droplets entered gelling bath, thereby accelerating gelation and promoting the formation of regular beads[12]. Similarly, studies confirmed that elevated temperature improved the sphericity of alginate-based hydrogel beads because of viscosity reduction[26]. However, when temperature was further increased to 8 °C, the gelation rate was declined to a minimum value (0.6391). This phenomenon occurred because too high temperature reduced the structural cohesiveness of droplets, impairing their ability to maintain shape integrity in the gelling bath[27].

To evaluate Tween's effect on gelation rate, various concentrations were tested (Table 1). Increasing Tween concentration from 0 to 2.0% progressively reduced the gelation rate from 0.9856 to 0.8076, indicating that the addition of Tween reduced the sphericity and gelation rate of the beads. Surfactants could destabilize bigel beads, which seemed to be contradictory to the empirical relationship that surfactants contributed to the formation of homogeneous and regular particles. Specifically, surfactant could diffuse into droplets, and fluidize or re-dissolve newly formed gel through broken intermolecular interaction of carrageenan, forming a sparse gel structure that was easy to collapse[28]. Furthermore, according to Samui et al.[29], surfactants like glycerol monostearate (GMS) could

Table 1. Single-factor experimental results of the gelation rate.

Factors	1	2	3	4	5
Ethanol concentration	0.3323 ± 0.0095	0.6511 ± 0.0145	0.8538 ± 0.0035	0.9693 ± 0.0089	0.8474 ± 0.0213
Gelling bath temperature	0.8418 ± 0.0191	0.9777 ± 0.0019	0.9844 ± 0.0037	0.9795 ± 0.0147	0.6391 ± 0.0099
Tween concentration	0.9856 ± 0.0099	0.9848 ± 0.0043	0.9431 ± 0.0047	0.8795 ± 0.0021	0.8076 ± 0.0758

Numbers 1 to 5 represent different levels of factors.

Table 2. Orthogonal array design and analysis on the gelation rate.

Sample runs	Factors			Gelation rate
	Ethanol concentration (%)	Gelling bath temperature (°C)	Tween concentration (%)	
1	50	−4	0	0.7799
2	50	0	0.5	0.8679
3	50	4	1	0.5948
4	75	−4	0.5	0.9727
5	75	0	1	0.9766
6	75	4	0	0.9483
7	100	−4	1	0.7685
8	100	0	0	0.9434
9	100	4	0.5	0.8276
k1	2.2426	2.5211	2.6716	
k2	2.8976	2.7879	2.6682	
k3	2.5395	2.3706	2.3399	
R	0.2184	0.1391	0.1106	
Rank	1	2	3	

interfere with the water/oil stability and induce oil leakage in bigels, which weakened the stabilization of gel structure and was harmful to gelation rate as well.

As shown in Table 2, the factors that influenced gelation rate were ranked as follows: ethanol concentration had the greatest effect, followed by bath temperature, and finally, Tween concentration. Gelling bath composed of 75% ethanol and 0% Tween at 0 °C effectively increased the gelation rate to 0.9882.

Effect of extrusion techniques on bigel beads

Analysis of single-factor experimental results

Figure 1a illustrates the effect of peristaltic pump rate on the sphericity of bigel beads. As the peristaltic pump rate was increased from 0.05 to 0.10 mL/min, the sphericity was improved from 0.95 to the highest value of 0.98. We found that at low rates (e.g., 0.05 mL/min), droplets exhibited a long residence time at the tip of the syringe needle. During this period, the emulsion temperature was decreased, which caused premature droplet solidification. This resulted in irregular bead shapes and frequent blockages of the needle tip, both of which contributed to the lower sphericity. In contrast, emulsions transported at a higher rate (0.10 mL/min) dripped smoothly, yielding beads with regular shapes. However, further increase in pump rate beyond 0.10 mL/min reduced the sphericity. This decline can be attributed to the increase in momentum of droplets caused by the very high velocity, leading to greater impact forces between the droplets and the gelling bath[12]. Consequently, droplets deformed more significantly, adversely affecting their spherical morphology. Based on these results, subsequent experiments used peristaltic pump rates between 0.05 and 0.15 mL/min.

Figure 1b depicts the influence of dripping height on the sphericity of bigel beads. The sphericity was increased from 0.90 to a maximum value of 0.96 as the height rose from 0.5 to 1.0 cm, but declined continuously as the height was further increased. Literature indicates that falling droplets would assume different shapes in three stages: tear shape, egg shape, and spherical shape[13]. At a shorter height (e.g., 0.5 cm), the droplets would detach in a tear-shaped form. This morphology was partially retained upon impact with the gelling bath, which yielded beads with distinct tails and reduced sphericity[12]. A longer falling distance allowed the surface tension to reshape the droplets toward attaining sphericity before impact, leading to the sphericity improvement at 1.0 cm. However, further increase in the falling distance (> 1.0 cm) imparted greater momentum to the droplets, and the resulting intensified impact with the gelling bath overcame stabilizing forces, causing pronounced shape deformation and consequent reduced sphericity[12,23]. Based on these findings, subsequent experiments used dripping heights between 0.5 and 1.5 cm.

Figure 1c shows the impact of transporting temperature on the sphericity of bigel beads. The sphericity was increased as the temperature was increased from 60 to 65 °C. This enhancement can be attributed to the delay in emulsion solidification caused by the higher temperature at the syringe needle tip, which facilitated droplet formation. However, temperatures exceeding 65 °C resulted in declined sphericity. This decline likely resulted from the decreased viscosity and consequent structural stability of the bigel at elevated temperatures[14,27], which impaired the ability of droplets to withstand impact forces upon contacting the gelling bath. Based on these results, the transporting temperature was set between 60 and 70 °C in subsequent experiments.

RSM model

RSM was applied using the BBD model. The test design combinations and their corresponding response values are listed in Table 3. The results illustrated that the sphericity of bigel beads ranged from 0.7525 to 0.9771. The highest sphericity (0.9771) was achieved under refined conditions: 0.10 mL/min pump rate, 1.0 cm height, and 65 °C.

The quadratic model for sphericity involving the various factors was expressed as follows:

$$\text{Sphericity} = -3.73427 - 0.590190A + 2.02845B + 0.116845C + 0.300144AB + 0.021199AC - 0.018889BC - 4.32229A^2 - 0.456464B^2 - 0.00078C^2$$

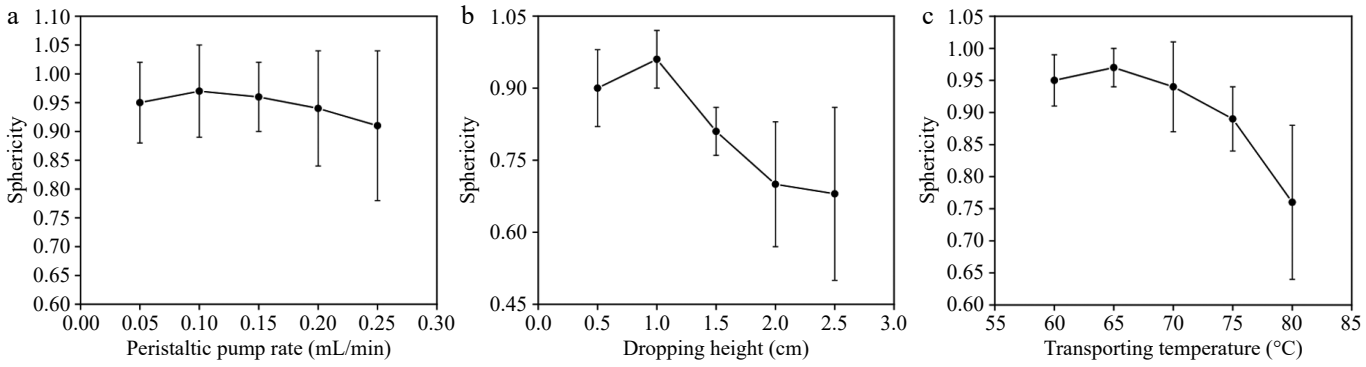

Fig. 1 Single factor experimental results for RSM.

https://doi.org/10.48130/fia-0026-0031

Table 3. Experimental runs, and coded factors with the experimental response factor in the application of response surface methodology (RSM).

Run	A, peristaltic pump rate (mL/min)	B, dropping height (cm)	C, transport temperature (°C)	Y, sphericity
1	0.05	0.5	65	0.8867
2	0.15	0.5	65	0.9010
3	0.05	1.5	65	0.7813
4	0.15	1.5	65	0.8256
5	0.05	1	60	0.9514
6	0.15	1	60	0.9562
7	0.05	1	70	0.9198
8	0.15	1	70	0.9457
9	0.1	0.5	60	0.8330
10	0.1	1.5	60	0.8532
11	0.1	0.5	70	0.9211
12	0.1	1.5	70	0.7525
13	0.1	1	65	0.9715
14	0.1	1	65	0.9771
15	0.1	1	65	0.9757
16	0.1	1	65	0.9671
17	0.1	1	65	0.9764

where A, B, and C represents the peristaltic pump rate, dripping height of emulsions, and transporting temperature, respectively. The absolute values of the coefficients in the equation directly reflect the influence of each factor on the indicator values[30]. A positive sign signifies a synergistic effect and a negative sign indicates an antagonistic effect of the variables[31]. Linear variables (B, C) and interaction terms (AB, AC) had a positive effect on sphericity, whereas the linear variable (A), other interaction term (BC), and second-order terms (A^2, B^2, C^2) had negative effects.

ANOVA was applied to confirm the reliability and suitability of the model (Table 4). The model was highly significant ($p < 0.0001$) with a nonsignificant lack of fit ($p = 0.0546 > 0.05$), indicating strong alignment between the regression and experimental data[32]. The predicted R^2 (0.9343) closely matched the adjusted R^2 (0.9888) as the difference between them was less than 0.2. This implied effective explanatory and predictive capabilities, and allowed the analysis and prediction of sphericity using this model[30,32]. The results showed that the linear terms A and B, the interaction term BC, and the quadratic terms B^2 and C^2 had a highly significant effect ($p < 0.01$). The linear term C and the quadratic term A^2 were significant ($p < 0.05$), while other variables lacked statistical significance. F-value analysis revealed that the order in which the factors affected the sphericity was dripping height (B) > peristaltic pump rate (A) > transporting temperature (C).

Figure 2a demonstrates the relationship between sphericity, dripping height, and transporting temperature at a constant peristaltic pump rate of 0.10 mL/min. When the dripping height was below 0.8 cm, the sphericity of bigel beads was increased with transporting temperature (from 60 to 70 °C). Conversely, heights exceeding 1.2 cm reduced the sphericity. These results highlighted the importance of adjusting the dripping height to maximize the sphericity. The elliptical contours in the 2D plot indicate significant interactions between the dripping height and transporting temperature[31]. This observation aligned with the ANOVA results (Table 4), which identified their interaction (term BC) as highly significant.

Figure 2b illustrates the effect of peristaltic pump rate and transporting temperature on sphericity at a fixed dripping height of 1.0 cm. The response surface exhibits a relatively flat slope, indicating negligible interaction between peristaltic pump rate and transporting temperature[33], which was consistent with the variance analysis results. Within optimal ranges, both increased pump rate and transporting temperature enhanced the sphericity of bigel beads. However, exceeding these thresholds reduced the sphericity, demonstrating the importance of parameter optimization.

Figure 2c depicts the relationship between sphericity, peristaltic pump rate, and dripping height at a constant transporting temperature of 65 °C. Sphericity was increased with dripping height up to 0.8 cm but decreased at greater heights. However, a minor difference was observed when the peristaltic pump rate was changed.

These results demonstrated that optimizing the peristaltic pump rate, dripping height, and transporting temperature improved the sphericity of bigel beads. Considering practical feasibility, the parameters were set to 0.13 mL/min (pump rate), 0.93 cm (dripping height), and 65 °C (transporting temperature). To evaluate the model's predictive accuracy, verification experiments were conducted under these optimized conditions. The resulting sphericity (0.9751) differed by only 1.59% from the predicted value, confirming strong model reliability and precision.

In subsequent study, bigel beads were prepared using an optimized gelling bath and extrusion techniques.

Table 4. Analysis of variance (ANOVA) for the fitted quadratic polynomial model for optimization of extraction parameters.

Source	Sum of squares	Degree of freedom	Mean square	*F*-Value	*p*-Value	Significance
Model	0.0831	9	0.0092	158.45	< 0.0001	**
A	0.001	1	0.0010	17.12	0.0044	**
B	0.0135	1	0.0135	232.08	< 0.0001	**
C	0.0004	1	0.0004	6.40	0.0393	*
AB	0.0002	1	0.0002	3.86	0.0901	NS
AC	0.0001	1	0.0001	1.93	0.2077	NS
BC	0.0089	1	0.0089	152.99	< 0.0001	**
A^2	0.0005	1	0.0005	8.43	0.0229	*
B^2	0.0548	1	0.0548	940.42	< 0.0001	**
C^2	0.0016	1	0.0016	27.48	0.0012	**
Residual	0.0004	7	0.0001			
Lack of fit	0.0003	3	0.0001	6.24	0.0546	NS
Pure error	0.0001	4	0			
Corresponding total	0.0836	16				
R^2	0.9951					
R^2 (adjusted)	0.9888					

Probability of *F*-test: ** $p < 0.01$; * $p < 0.05$; NS, nonsignificant difference.

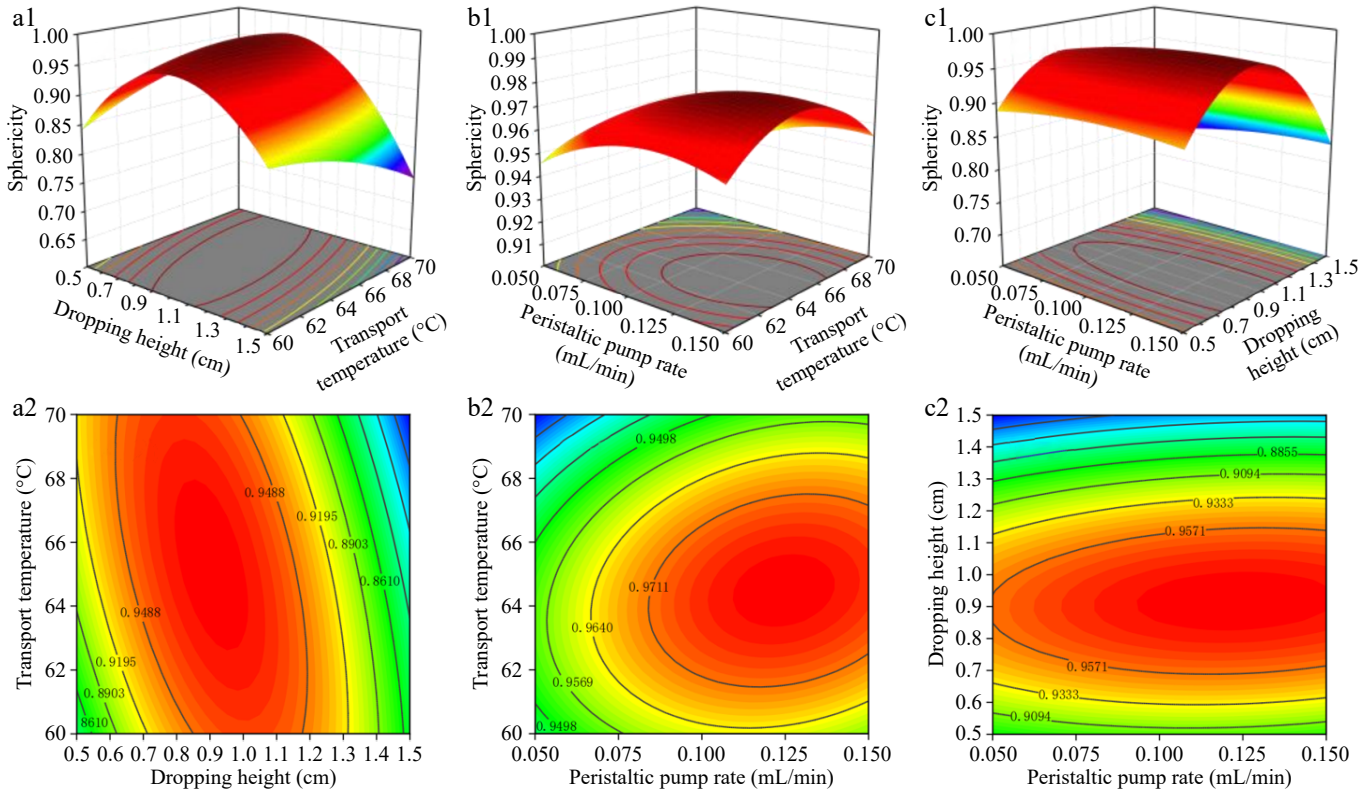

Fig. 2 Three-dimensional response surface and corresponding two-dimensional contour plots.

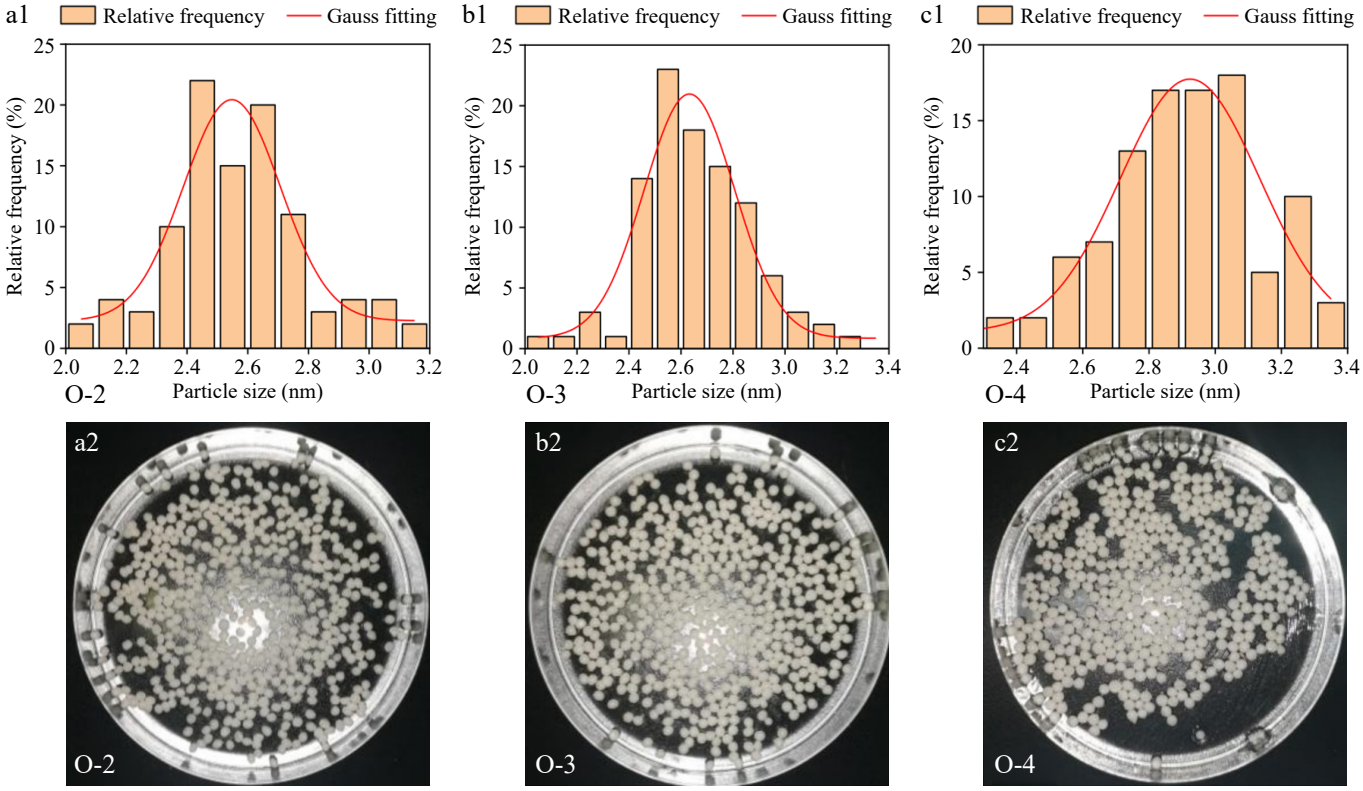

Fig. 3 Appearance and size distributions of bigel beads.

Characterization of bigel beads

Appearance and microstructures of the bigel beads

Figures 3 and 4 show the appearance and size distributions of bigel beads. O-2 had a sphericity of 0.85 and showed an inhomogeneous size distribution with the smallest average diameter (2.57 mm). As the oil-phase proportion was increased, sphericity was significantly increased and size distribution was sharpened, and the maximum sphericity (0.94) and largest average diameter

https://doi.org/10.48130/fia-0026-0031

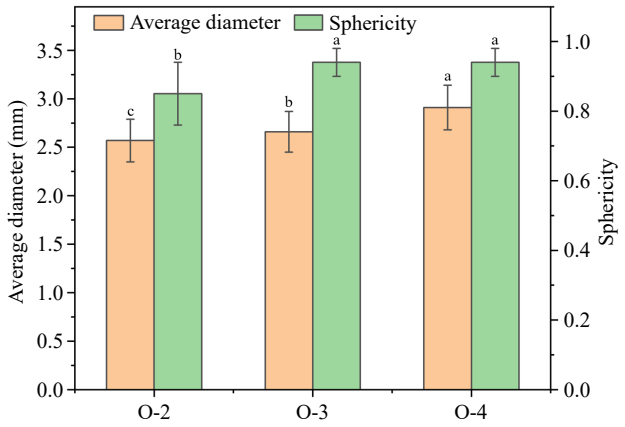

Fig. 4 Average diameter and sphericity of bigel beads. Different lowercase letters in the same row indicate significant differences ($p < 0.05$).

(2.91 mm) were reached in O-4. These results suggested that higher oil content increased both the sphericity and particle size of bigel beads. According to Yang et al.[9], oleogel-rich emulsions exhibited substantially higher viscosity. Such elevated viscosity helped the droplets overcome the impact forces upon contacting the gelling bath, maintaining a spherical morphology and thereby improving the sphericity[12]. Relevant literature also confirmed that higher viscosity could lead to larger diameter of alginate-based beads[34].

Confocal laser scanning microscope (CLSM) observation revealed the microstructural evolution of bigel beads as the oil content was increased (Fig. 5). O-2 exhibited an oleogel-in-hydrogel structure characterized by finely dispersed oil droplets with small size. Increasing the oil phase to 30% induced obvious droplet coalescence and larger oil domains, consistent with literature findings that higher oil proportion led to larger mean droplet size and closer packing of droplets[35]. When the oleogel concentration reached 40%, the oil phase became continuous and the two phases mutually interpenetrated. The absence of a distinct dispersed phase indicated the development of bi-continuous structures[3].

Mechanical properties of the bigel beads

Texture analysis was conducted to evaluate the mechanical properties of bigel beads. As shown in Fig. 6, the lowest hardness was observed in O-2 (0.17 N). As the oleogel fraction was increased from 20% to 40%, hardness progressively increasedto the maximum value (0.22 N). These results indicated that a higher oleogel content increased the hardness and degree of structuration of bigel beads.

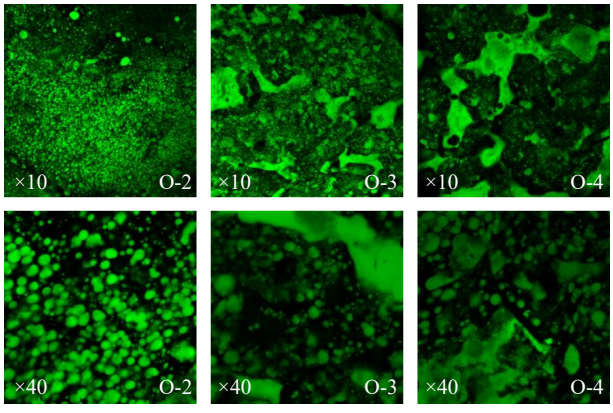

Fig. 5 Microstructure of bigel beads.

Such enhancements in the mechanical properties of the bigel systems can be attributed to the reinforcement of the entire network caused by the interaction between the oil phase and gelled water droplets trapped in the matrix, which strengthened the gel[3,8,36]. Samui et al.[29] also reported that the hardness of bigels containing gelatin hydrogels and GMS oleogels was enhanced with the increase in oleogel ratio.

Cohesiveness reflects the ability of bigel beads to maintain structural integrity against deformation, indicating internal bond strength and post-deformation structural stability[37,38]. Increasing the oleogel percentage from 30% to 40% significantly enhanced the cohesiveness from 0.36 to 0.62 (an increase of 72.2%), indicating improved three-dimensional network formation and consistency[39]. This enhancement stemmed from the strengthened attractive forces between the hydrogel and oleogel phases and strong interactions between the oleogelator molecules, especially at higher oil-phase concentrations[40]. Similarly, Shahid et al.[41] reported an increase in the cohesiveness of GMS-bakla starch bigels from 36.06 to 100.51 with increase in oleogel content. Notably, no significant difference in cohesiveness was observed as the oil-phase fraction was increased from 20% to 30%. This threshold effect was likely because of the insufficient network reinforcement below 30% oleogel concentration.

Simulated oral processing and digestion

Tribological characterization of the bigel beads

The tribological properties of bigel beads during simulated oral processing were evaluated using saliva–yogurt systems (containing 6% [w/w] and 10% [w/w] bigel beads, respectively), which were selected because of the good taste and consumer acceptance of yogurt containing gel beads. As shown in Fig. 7, all samples exhibited classical Stribeck curves with distinct boundary, mixed, and hydrodynamic regions, consistent with the tribological behavior reported for glucomannan–gelatin/stearic acid bigels[20]. In the boundary region, the friction was dependent on the properties of the lubricating film and the surface asperities rather than the entrainment speed. Higher friction coefficients were observed because it was difficult to entrain the bigel fragments after homogenization into the contact surfaces at such low sliding speed to form a lubricating film layer on the surface[41]. In the mixed regime, increasing sliding speed reduced friction coefficients to minimum values. Relevant literature has confirmed that negative pressure between plates improves sample entrainment to form a lubricating film, consequently reducing frictions. As the sliding speed continued to

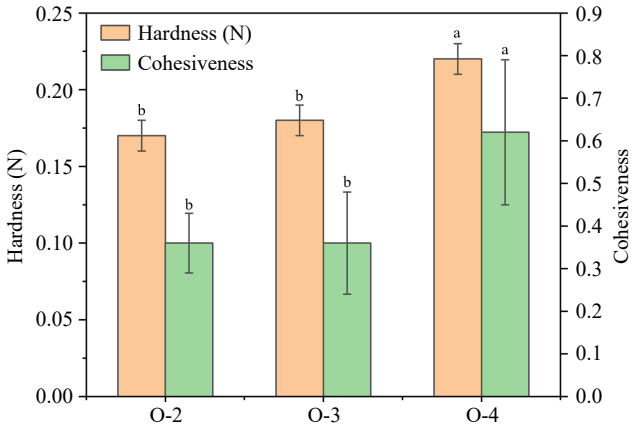

Fig. 6 Mechanical properties of bigel beads. Different lowercase letters in the same row indicate significant differences ($p < 0.05$).

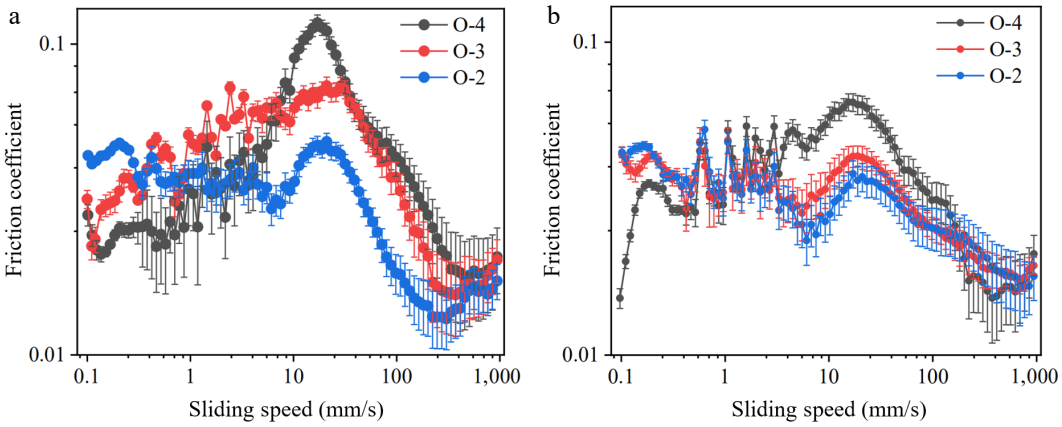

Fig. 7 Tribological properties of bigel beads. (a) 6% (w/w) and (b) 10% (w/w) bigel beads were added to yoghurt, respectively.

rise (> 200 mm/s), friction coefficients were increased as the tribological behavior entered the hydrodynamic region[19]. At this stage, the tribological behavior was governed by the rheology of mixtures (oil droplets, saliva, and yogurt) entrained into the contact surfaces[17]. The friction coefficients were increased because of the adhesion of mucin/other saliva proteins on the PDMS surface and the higher viscosity due to the tightly packed droplets[17,19,41].

The friction coefficients at 20 mm/s (F_{20}) and 100 mm/s (F_{100}) represented low and high chewing intensity scenarios, respectively[42]. Notably, both F_{20} and F_{100} were increased with higher oleogel percentage, indicating that greater friction correlated with increased oil content. This aligned with our previous finding that elevated oleogel content increased system viscosity[9]. Viscous systems exhibited greater interfacial resistance during sliding and, consequently, higher friction coefficients[19], which led to a potential sticky sensation.

In vitro *digestion behavior of the bigel beads*

As shown in Fig. 8, after 10 min of processing in artificial saliva, all bigel samples retained intact structures with clear surrounding solutions. Minimal FFA was released due to the short oral residence (Fig. 9). During SGF digestion, significant bead swelling and fragmentation occurred. O-4 samples were completely degraded and no intact gel structures were observed after a 1-h SGF digestion, yielding turbid fluid from undigested oil and mixed micelles[43]. O-2 and O-3 partially maintained spherical structures with discernible boundaries. Flocculated and aggregated clusters of the samples were observed after digestion, indicating partial disintegration of the gel network[43]. Such difference in structure stability can be attributed to the strengthening of networks against gastric conditions by the higher carrageenan content (in the water-rich O-2 and O-3)[44], thereby leading to lighter structural deformation. O-4 exhibited the highest gastric FFA release (10.42%). Gel network fragmentation and deformation could influence the release of FFA[9]. In appearance, O-4 had the most severe structural damage, which allowed further contact between the oil droplets and pancreatic lipase[45], consequently resulting in the highest FFA release percentage.

After approximately 2 h in SIF, all beads showed complete structural disintegration with no residual gel clumps, indicating substantial network disruption. This was in line with the study of Liu et al.[44], confirming severe structural damage during SIF digestion.

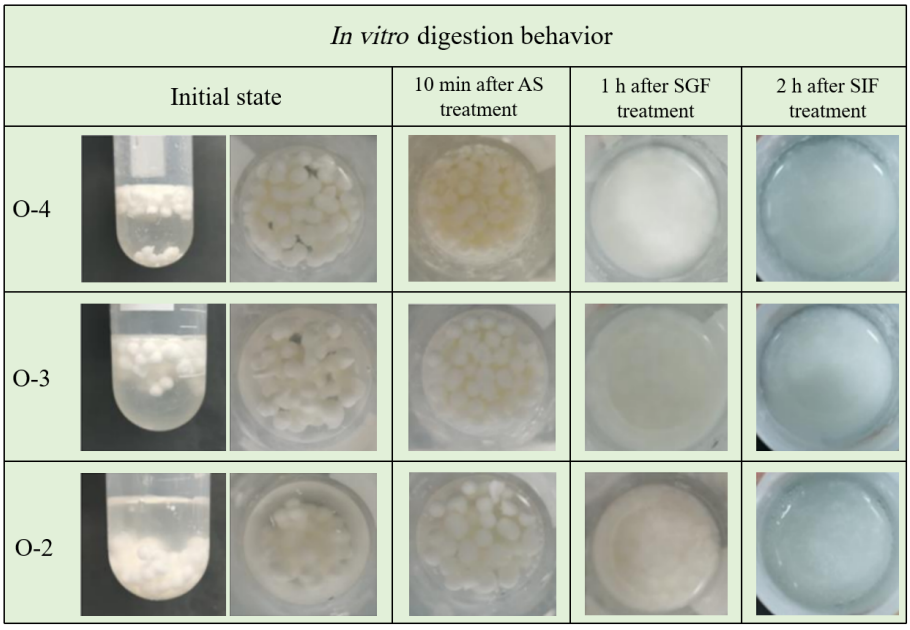

Fig. 8 *In vitro* digestion behavior of bigel beads. AS, SGF, and SIF stand for artificial saliva, simulated gastric fluid, and simulated intestinal fluid, respectively.

https://doi.org/10.48130/fia-0026-0031

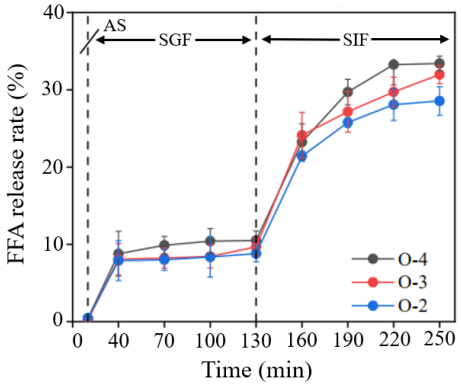

Fig. 9 *In vitro* free fatty acid release profile of bigel beads. AS, SGF, and SIF represent artificial saliva, simulated gastric fluid, and simulated intestinal fluid, respectively.

FFA release during SIF digestion featured an initial rapid surge followed by a slower release. Notably, O-4 exhibited the highest cumulative FFA release (33.40%). This increased release resulted from two key factors: (1) pancreatic lipase required diffusion through the hydrogel network to access the oil droplets[45], and (2) the hydrogel phase inherently retarded the lipolysis reaction by impeding lipase–oil contact[20]. As shown in the microstructure observation, the structure of O-4 transitioned from O/W to bi-continuous ("Appearance and microstructures of the bigel beads"), which weakened the protective barrier of the hydrogel at lower hydrogel contents. This facilitated enzyme diffusion into the hydrogel matrix and FFA diffusion out of the matrix[11,43], explaining the elevated FFA release of O-4. These results underscored the hydrogel network's critical role as a diffusion barrier[45].

Conclusions

In this study, we reported the optimization of the preparation process of bigel beads through the integration of orthogonal experiments and RSM. By optimizing the gelling bath parameters and extrusion techniques, we significantly enhanced both the gelation efficiency and sphericity of bigel beads. Notably, the oil–water phase ratio exerted a profound influence on bead structure, physicochemical properties, and performance during simulated oral processing and gastrointestinal digestion. An increased oil-phase proportion led to larger particle size, improved sphericity, greater hardness, and enhanced cohesiveness. These structural modifications, in turn, elevated frictional interactions during simulated mastication while compromising the bead's structural stability, ultimately resulting in a significantly accelerated release of free fatty acids. This work provides novel insights into the fabrication protocols and structure–function relationships of bigel beads. Future investigations may focus on integrating these beads into complex food matrices and evaluating the bioavailability of encapsulated bioactive compounds.

Ethical statements

Not applicable.

Author contributions

The authors confirm their contributions to the paper as follows: writing – original draft, software: Zhao Y; conceptualization, data curation, and investigation: Song J; methodology: Yang J; visualization: Jin Y; formal analysis: Li G; supervision and software: Liu J; writing – review and editing, supervision, project administration, and funding acquisition: Mao L. All authors reviewed the results and approved the final version of the manuscript.

Data availability

The datasets generated during and/or analyzed during the current study are available from the corresponding author upon reasonable request.

Acknowledgments

The research was funded by National Natural Science Foundation of China (No. 32272471) and Cross-disciplinary Innovation in Food Flavor and Health of Beijing Technology and Business University in 2025 (FFHCI-2025004).

Declaration of competing interest

The authors declare that they have no known competing financial interests or personal relationships that could have appeared to influence the work reported in this paper.

Supplementary information accompanies this paper online at: https://doi.org/10.48130/fia-0026-0031.

Dates

Received 18 January 2026; Revised 3 April 2026; Accepted 13 May 2026; Published online 28 July 2026

References

[1] Shakeel A, Lupi FR, Gabriele D, Baldino N, De Cindio B. 2018. Bigels: a unique class of materials for drug delivery applications. *Soft Materials* 16(2):77–93

[2] Mao L, Lu Y, Cu, M, Miao S, Gao Y. 2020. Design of gel structures in water and oil phases for improved delivery of bioactive food ingredients. *Critical Reviews in Food Science and Nutrition* 60(10):1651–1666

[3] Zheng H, Mao L, Cui M, Liu J, Gao Y. 2020. Development of food-grade bigels based on κ-carrageenan hydrogel and monoglyceride oleogels as carriers for β-carotene: roles of oleogel fraction. *Food Hydrocolloids* 105:105855

[4] Lee GR, Baek Y, Jeong E, Lee HG. 2024. Development and characterization of a novel bigel system based on candelilla wax oleogel and guar gum hydrogel for heat-triggered release properties. *Food Hydrocolloids* 152:109892

[5] Zhou M, Li B, Wu A, Li J, Tang J, et al. 2025. Gelatin-wax-based bigel system: innovative research on a low-calorie fat substitute. *Lwt* 224:117836

[6] Moguiliansky S, Friedman N, Davidovich-Pinhas M. 2025. The effect of transglutaminase on the structure and texture of plant-protein based bigel. *Food Hydrocolloids* 162:110981

[7] Fernandes Almeida R, Aguiar Borges L, Torres da Silva T, Serafim Timóteo Dos Santos N, Gianasi F, et al. 2024. Chocolates, compounds and spreads: a review on the use of oleogels, hydrogels and hybrid gels to reduce saturated fat content. *Food Research International* 178:113986

[8] Martins AJ, Guimarães A, Fuciños P, Sousa P, Venâncio A, et al. 2023. Food-grade bigels: evaluation of hydrogel:oleogel ratio and gelator concentration on their physicochemical properties. *Food Hydrocolloids* 143:108893

[9] Yang J, Song J, Miao S, Gao Y, Mao L. 2024. Alginate-based gel beads with bigel structures: preparation, characterization and bioactive encapsulation. *Food Hydrocolloids* 146(Part B):109294

[10] Saqib MN, Khaled BM, Liu F, Zhong F. 2022. Hydrogel beads for designing future foods: structures, mechanisms, applications, and challenges. *Food Hydrocolloids for Health* 2:100073

[11] Lin Q, Li X, McClements DJ, Jin Z, Qiu C, et al. 2024. Plant-based delivery systems for controlled release of hydrophilic and hydrophobic active ingredients: pea protein-alginate bigel beads. *Food Hydrocolloids* 154:110101

[12] Chan ES, Lee BB, Ravindra P, Poncelet D. 2009. Prediction models for shape and size of ca-alginate macrobeads produced through extrusion–dripping method. *Journal of Colloid and Interface Science* 338(1):63–72

[13] Lee BB, Ravindra P, Chan ES. 2013. Size and shape of calcium alginate beads produced by extrusion dripping. *Chemical Engineering & Technology* 36(10):1627–1642

[14] Jeong C, Kim S, Lee C, Cho S, Kim SB. 2020. Changes in the physical properties of calcium alginate gel beads under a wide range of gelation temperature conditions. *Foods* 9(2):180

[15] Lu J, Zamaratskaia G, Langton M, Rohnisch HE, Karkehabadi S. 2024. Minimizing anti-nutritional factors in wet protein extraction from Swedish faba beans through the application of response surface methodology. *Food Chemistry* 460(Part 2):140700

[16] Wang Y, Han L. Yu W, Zhao W, Pan J, et al. 2023. Carrageenan addition improves the melting temperature and 3D printing performance of the gelatin system. *Food Hydrocolloids* 144:108918

[17] Zhang Y, Zhang R, Lu Y, Gao Y, Mao L. 2024. Effect of simulated saliva on rheological and tribological properties of oleogel-in-water HIPEs during oral processing. *Journal of Colloid and Interface Science* 653(Part B):1018–1027

[18] Krop EM, Hetherington MM, Holmes M, Miquel S, Sarkar A. 2019. On relating rheology and oral tribology to sensory properties in hydrogels. *Food Hydrocolloids* 88:101–113

[19] Zhang Y, Zhang R, Ying J, Li S, Gao Y, et al. 2024. Tailoring microstructures of oleogel-based HIPEs to modulate oral processing properties: rheology, tribology and mastication effects. *Food Hydrocolloids* 153:109968

[20] Tian W, Huang Y, Liu L, Yu Y, Cao Y, et al. 2024. Tailoring the oral sensation and digestive behavior of konjac glucomannan-gelatin binary hydrogel based bigel: effects of composition and ratio. *International Journal of Biological Macromolecules* 256(Part 1):127963

[21] Cassanelli M, Norton I, Mills T. 2017. Effect of alcohols on gellan gum gel structure: bridging the molecular level and the three-dimensional network. *Food Structure* 14:112–120

[22] Yang D, Yang H. 2020. Effects of ethanol on gelation of iota-carrageenan. *LWT* 126:109281

[23] Davarcı F, Turan D, Ozcelik B, Poncelet D. 2017. The influence of solution viscosities and surface tension on calcium-alginate microbead formation using dripping technique. *Food Hydrocolloids* 62:119–127

[24] Tong C, Liu L, Lin Q, Liu J, Xue Q, et al. 2022. Insights into the formation of konjac glucomannan gel induced by ethanol equilibration. *Food Hydrocolloids* 126:107469

[25] Motin MA, Kabir MH, Huque ME. 2005. Viscosities and excess viscosities of methanol, ethanol and *n*-propanol in pure water and in water + surf excel solutions at different temperatures. *Physics and Chemistry of Liquids* 43(2):123–137

[26] Bennacef C, Desobry-Banon S, Probst L, Desobry S. 2021. Advances on alginate use for spherification to encapsulate biomolecules. *Food Hydrocolloids* 118:106782

[27] Richa, Roy Choudhury A. 2023. Self-assembled pH-stable gellan/*κ*-carrageenan bigel: rheological studies and viscosity prediction by neural network. *International Journal of Biological Macromolecules* 237:124057

[28] Lapitsky Y, Kaler EW. 2004. Formation of surfactant and polyelectrolyte gel particles in aqueous solutions. *Colloids and Surfaces A: Physicochemical and Engineering Aspects* 250(1–3):179–187

[29] Samui T, Goldenisky D, Rosen-Kligvasser J, Davidovich-Pinhas M. 2021. The development and characterization of novel in-situ bigel formulation. *Food Hydrocolloids* 113:106416

[30] Zhang C, Ding W, Mamattursun A, Ma X, Qi S, et al. 2025. Optimization of enzyme-ultrasound assisted extraction from mulberries anthocyanins based on response surface methodology and deep neural networks and analysis of *in vitro* antioxidant activities. *Food Chemistry* 478:143597

[31] Mohajeri M, Mokhtari S, Khandan M, Ayatollahi SA, Kobarfard F, et al. 2025. Enhancing polyamine enrichment from wheat germs: a study utilizing response surface methodology and liquid chromatography-mass spectrometry. *Food Chemistry* 463(Part 3):141408

[32] Zheng J, Zhao L, Zhang J, Sheng X. 2025. Effect of cold plasma on ochratoxin A detoxification: response surface, degradation pathways, and cytotoxicity analysis. *Food Chemistry* 477:143595

[33] Anoraga SB, Shamsudin R, Hamzah MH, Sharif S, Saputro AD, et al. 2024. Optimization of subcritical water extraction for pectin extraction from cocoa pod husks using the response surface methodology. *Food Chemistry* 459:140355

[34] Berninger T, Mitter B, Preininger C. 2016. The smaller, the better? The size effect of alginate beads carrying plant growth-promoting bacteria for seed coating. *Journal of Microencapsulation* 33:127–136

[35] Saffold AC, Acevedo NC. 2021. Development of novel rice bran wax/gelatin-based biphasic edible gels and characterization of their microstructural, thermal, and mechanical properties. *Food and Bioprocess Technology* 14(3):2219–2230

[36] Shahid A, Kumar KJ. 2025. Bakla starch-based bigels as low-calorie fat replacers: influence of hydrogel ratio. *Food Biophysics* 20:49

[37] Eisinaitė V, Jasutienė I, Vinauskienė R, Leskauskaitė D. 2022. Development of bigel based dysphagia-oriented products, structured with collagen and carnauba wax: characterisation and rheological behaviour. *International Journal of Food Science & Technology* 58(1):145–153

[38] Shakouri S, Arabshahi S, Madanchi H, Mohammadifar MA, Abdolshahi A. 2024. Effect of carboxymethyl cellulose incorporation to gelatin-sunflower oil bigel on the physicochemical and structural properties. *Polymers for Advanced Technologies* 35(9):e6567

[39] Mata-Mota JD, Gallegos-Infante JA, Pérez-Martínez JD, Rocha-Guzmán NE, González-Laredo RF. 2023. Effect of hydrogel/oleogel ratio, speed and time of mixing, on the mechanical properties of bigel materials and the application of Cox-Merz rule. *Food Materials Research* 3:24

[40] Shakouri S, Tehrani MM, Koocheki A, Farhoosh R, Abdolshahi A. 2025. The development and characterization of edible bigel a hydrogel/oleogel structure based on guar gum, walnut oil and rice bran wax for using as fat replacer. *Journal of Polymers and the Environment* 33:2058–2071

[41] Zhang Y, Wang Y, Zhang R, Yu J, Gao Y, et al. 2022. Tuning the rheological and tribological properties to simulate oral processing of novel high internal phase oleogel-in-water emulsions. *Food Hydrocolloids* 131:107757

[42] Tian W, Huang Y, Song Z, Abdullah, Yu Y, et al. 2023. Flexible control of bigel microstructure for enhanced stability and flavor release during oral consumption. *Food Research International* 174(Part 1):113606

[43] Zhang R, Yang J, Li J, Gao Y, Mao L. 2025. Modification of the interface of oleogel-hydrogel bigel beads for enhanced stability and prolonged release of bioactives. *Food Chemistry* 468:142448

[44] Liu L, Wang W, Duan S, Liu J, Mo J, et al. 2024. Novel pickering bigels stabilized by whey protein microgels: interfacial properties, oral sensation and gastrointestinal digestive profiles. *Food Research International* 188:114352

[45] Liu G, Wang Y, Yang J, Wang Y, He H, et al. 2025. Roles of different polysaccharides on the structures of alginate-based Bigel beads and co-delivery of bioactives. *Food Chemistry: X* 27:102359